

Revisit of Tension in Recent SNIa Datasets

Miao Li,^{1,2,3,*} Xiao-Dong Li,^{4,1,†} and Shuang Wang^{5,1,‡}

¹*Institute of Theoretical Physics, Chinese Academy of Sciences, Beijing 100080, China*

²*Kavli Institute for Theoretical Physics China, Chinese Academy of Sciences, Beijing 100080, China*

³*Key Laboratory of Frontiers in Theoretical Physics,
Chinese Academy of Sciences, Beijing 100080, China*

⁴*Interdisciplinary Center for Theoretical Study, University of Science and Technology of China, Hefei 230026, China*

⁵*Department of Modern Physics, University of Science and Technology of China, Hefei 230026, China*

Although today there are many observational methods, Type Ia supernovae (SNIa) is still one of the most powerful tools to probe the mysterious dark energy (DE). The most recent SNIa datasets are the 307 SNIa “Union” dataset [Kowalski et al. 2008] and the 397 SNIa “Constitution” dataset [Hicken et al. 2009]. In a recent work [Wei 2010], Wei pointed out that both Union and Constitution datasets are in tension with the observations of cosmic microwave background (CMB) and baryon acoustic oscillation (BAO), and suggested that two truncated versions of Union and Constitution datasets, namely “UnionT” and “ConstitutionT”, should be used to constrain various DE models. But in [Wei 2010], only the Λ CDM model is used to select the outliers from the Union and the Constitution dataset. In principle, since different DE models may select different outliers, the truncation procedure should be performed for each different DE model. In the present work, by performing the truncation procedure of [Wei 2010] for 10 different models, we demonstrate that the impact of different models is negligible, and the approach adopted in [Wei 2010] is valid. Moreover, by using the 4 SNIa datasets mentioned above, as well as the observations of CMB and BAO, we perform best-fit analysis on the 10 models. It is found that: (1) For each DE model, the truncated SNIa datasets not only greatly reduce χ^2_{min} and χ^2_{min}/dof , but also remove the tension between SNIa data and other cosmological observations. (2) The CMB data is very helpful to break the degeneracy among different parameters, and plays a very important role in distinguishing different DE models. (3) The current observational data are still too limited to distinguish all DE models.

I. INTRODUCTION

Observations of Type Ia supernovae (SNIa) [Riess et al. 1998, Perlmutter et al. 1999, Tonry et al. 2003, Knop et al. 2003, Riess et al. 2004a], cosmic microwave background (CMB) [Bennet et al. 2003, Spergel et al. 2003, Spergel et al. 2007, Page et al. 2007, Hinshaw et al. 2007, Komatsu et al. 2009] and large scale structure (LSS) [Tegmark et al. 2004a, Tegmark et al. 2004b, Tegmark et al. 2006] all indicate the existence of dark energy (DE) driving the current accelerating expansion of the universe. The most obvious theoretical candidate of DE is the cosmological constant Λ , but it is plagued with the fine-tuning problem and the coincidence problem [Weinberg 1989, Weinberg 2000, Sahni and Starobinsky 2000, Carroll 2001, Peebles and Ratra 2003, Padmanabhan 2003, Copeland et al. 2006]. There are also many dynamical DE models, such as quintessence [Peebles and Ratra 1988, Ratra and Peebles 1988, Ratra and Peebles 1988, Zlatev et al. 1999], phantom [Caldwell 2002, Carroll et al. 2003], k -essence [Armendariz-Picon et al. 1999, Chiba et al. 2000, Armendariz-Picon et al. 2001], CPL [Chevallier and Polarski 2001, Linder 2003], tachyon [Padmanabhan 2002, Bagla et al. 2003], hessence [Wei et al. 2005, Wei and Cai 2005], Chaplygin gas [Kamenshchik et al. 2001], generalized Chaplygin gas [Bento et al. 2002], holographic [Li 2004, Huang and Li 2005a, Huang and Li 2005b, Li et al. 2008, Li et al. 2009a, Zhang 2010], agegraphic [Wei and Cai 2008a, Wei and Cai 2008b], holographic Ricci [Gao et al. 2009], Yang-Mills condensate [Zhang et al. 2007, Xia and Zhang 2007, Wang et al. 2008, Wang and Zhang 2008], etc. Although numerous theoretical models have been proposed in the past decade, the nature of DE still remains a mystery.

In recent years, the numerical study of DE, i.e. utilizing cosmological observations to constrain DE models, has become one of the most active fields in the modern cosmology [Albrecht et al. 2006, Wang 2000, Wang and Mukherjee 2004, Wang and Mukherjee 2007, Huterer and Starkman 2003, Huterer and Cooray 2005, Huang and Gong 2004, Zhang and Wu 2004, Zhang 2005, Chang et al. 2006, Zhang 2007, Zhang and Wu 2007,

*Electronic address: mli@itp.ac.cn

†Electronic address: renzhe@mail.ustc.edu.cn

‡Electronic address: swang@mail.ustc.edu.cn

Zhang 2009, Wang et al. 2005, Wang et al. 2006, Ma et al. 2009a, Ma et al. 2009b, Wei and Cai 2007, Wei and Cai 2008c, Wei and Cai 2009]. Although today there are many observational methods, SNIa is still one of the most powerful tools to probe the mysterious DE. In the past decade, many SNIa datasets, such as Gold04 [Riess et al. 2004b], Gold06 [Riess et al. 2007], SNLS [Astier et al. 2007], ESSENCE [Wood-Vasey et al. 2007], Davis [Davis et al. 2007], have been released, while the number and quality of SNIa have continually increased. The most recent SNIa datasets are “Union” [Kowalski et al. 2008] and “Constitution” [Hicken et al. 2009], and they have been widely used in the literature [Shafieloo et al. 2009, Li et al. 2009b, Qi et al. 2009, Huang et al. 2009, Zhang and Wu 2009, Chen et al. 2009, Gong and Li 2010a, Gong et al. 2010b, Sanchez et al. 2009, Mortonson et al. 2009, Wang et al. 2010]. However, these SNIa datasets are not always consistent with other types of cosmological observations, and are even in tension with other SNIa samples. For examples, in [Jassal et al. 2005, Jassal et al. 2006, Nesseris and Perivolaropoulos 2005], the Gold04 dataset was shown to be inconsistent with the SNLS dataset: the SNLS dataset favors the Λ CDM model, while the Gold04 dataset favors the dynamical DE model. In [Nesseris and Perivolaropoulos 2007], by comparing the maximum likelihood fits of the CPL parameters (w_0, w_1) given by different SNIa samples, Nesseris and Perivolaropoulos found that the Gold06 dataset is also in 2σ tension with the SNLS dataset. Moreover, they also investigated how to remove this tension. The method is simple. First, they fitted the Λ CDM model to the whole 182 SNIa in the Gold06 dataset, and obtained the best-fit parameter value of Λ CDM model (for SNIa data only). Then, they calculated the relative deviation to the best-fit Λ CDM prediction, $|\mu_{obs} - \mu_{\Lambda CDM}|/\sigma_{obs}$, for all the 182 data points. Here μ_{obs} is the observational value of distance modulus, $\mu_{\Lambda CDM}$ is the theoretical value of distance modulus given by the best-fit Λ CDM model, and σ_{obs} is the 1σ error of distance modulus. By searching the SNIa samples satisfying $|\mu_{obs} - \mu_{\Lambda CDM}|/\sigma_{obs} > 1.8$, they isolated six SNIa that are mostly responsible for the tension. Further, by using the random truncation method, they demonstrated that these 6 SNIa are systematically different from the Gold06 dataset.

In a recent work, by comparing the maximum likelihood fits of the CPL parameters (w_0, w_1), Wei [Wei 2010] pointed out that both Union and Constitution dataset are also in tension with the observations of CMB and baryon acoustic oscillation (BAO). Moreover, he also investigated how to remove these tensions. By using the method of truncation of [Nesseris and Perivolaropoulos 2007], Wei found out the main sources that are responsible for the tensions: for the Union set, there are 21 SNIa differing from the best-fit Λ CDM prediction beyond 1.9σ (i.e. $|\mu_{obs} - \mu_{\Lambda CDM}|/\sigma_{obs} > 1.9$); and for the Constitution set, there are 34 SNIa differing from the best-fit Λ CDM prediction beyond 1.9σ . The specific limit of truncation (i.e. 1.9σ) is chosen based on two considerations: first, the tension between SNIa samples and other observations can be completely removed; second, the number of usable SNIa can be preserved as much as possible (see [Wei 2010] for details). By subtracting these outliers from the Union dataset and the Constitution dataset, respectively, two new SNIa datasets, “UnionT” and “ConstitutionT” (“T” stands for “truncated”), were obtained. Further, Wei argued that the UnionT and the ConstitutionT datasets are fully consistent with the other cosmological observations, and should be used to constrain various DE models. But in [Wei 2010], only the Λ CDM model is used to select the outliers from the Union and the Constitution dataset. Since different DE models may select different outliers, one may doubt whether the approach adopted in [Wei 2010] is valid. In principle, the truncation procedure should be performed for each different DE model. Only if the impact of different models is negligible, one can conclude that the conclusion of Wei is correct. So in the present work, we shall consider 10 different models. The truncation procedure will be performed for all these 10 models, and the corresponding cosmological consequences will be explored.

This paper is organized as follows: In Section 2, we briefly describe 10 theoretical models considered in this work. In Section 3, we present the method of data analysis, as well as the SNIa datasets we used in this paper. By performing the truncation procedure of [Wei 2010] for 10 different models, we demonstrate that the approach adopted in [Wei 2010] is valid. In Section 4, we show the data fitting results of 10 models, and present the corresponding conclusions. Section 5 is a short summary. In this work, we assume today’s scale factor $a_0 = 1$, so the redshift z satisfies $z = a^{-1} - 1$; the subscript “0” always indicates the present value of the corresponding quantity, and the unit with $c = \hbar = 1$ is used.

II. MODELS

For a spatially flat (the assumption of flatness is motivated by the inflation scenario) Friedmann-Robertson-Walker (FRW) universe with matter component ρ_m and DE component ρ_{de} , the Friedmann equation reads

$$3M_{Pl}^2 H^2 = \rho_m + \rho_{de}, \quad (1)$$

where $M_{Pl} \equiv 1/\sqrt{8\pi G}$ is the reduced Planck mass, and $H \equiv \dot{a}/a$ is the Hubble parameter. Using this formula, one can easily get

$$E(z) \equiv H(z)/H_0 = [\Omega_{m0}(1+z)^3 + (1 - \Omega_{m0})f(z)]^{1/2}, \quad (2)$$

where H_0 is the Hubble constant, Ω_{m0} is the present fractional matter density, and key function $f(z) \equiv \rho_{de}(z)/\rho_{de}(0)$ is given by the specific DE model. Equivalently, we have

$$E(z) = \left(\frac{\Omega_{m0}(1+z)^3}{1 - \Omega_{de}} \right)^{1/2}, \quad (3)$$

where $\Omega_{de} \equiv \frac{\rho_{de}}{\rho_c} = \frac{\rho_{de}}{3M_{Pl}^2 H^2}$ is the fractional DE density. Clearly, different DE model will give different $E(z)$. In the following, we shall briefly describe the models considered in this work.

A. Single-parameter models

(1) The Λ CDM model: The DE density is always a constant, i.e. the equation of state (EOS) $w = -1$, so

$$E(z) = \sqrt{\Omega_{m0}(1+z)^3 + (1 - \Omega_{m0})}. \quad (4)$$

(2) The Dvali-Gabadadze-Porrati (DGP) model: For this modified gravity model, the form of $E(z)$ is [Dvali et al. 2000]

$$E(z) = \sqrt{\Omega_{m0}(1+z)^3 + \Omega_{rc}} + \sqrt{\Omega_{rc}}, \quad (5)$$

where Ω_{rc} is a constant, satisfies

$$\Omega_{rc} = \left(\frac{1 - \Omega_{m0}}{2} \right)^2. \quad (6)$$

(3) The agegraphic dark energy (ADE): The DE density is characterized by the conformal age η of the universe [Wei and Cai 2008b],

$$\rho_{de} = 3n^2 M_{Pl}^2 \eta^{-2}, \text{ and } \eta \equiv \int \frac{dt}{a} = \int \frac{da}{a^2 H}, \quad (7)$$

where n is a positive constant. The equation of motion for Ω_{de} is given by [Wei and Cai 2008b]

$$\frac{d\Omega_{de}}{dz} = -\Omega_{de}(1 - \Omega_{de}) \left[3(1+z)^{-1} - \frac{2}{n} \sqrt{\Omega_{de}} \right]. \quad (8)$$

As in [Wei and Cai 2008b], we choose the initial condition, $\Omega_{de}(z_{ini}) = n^2(1+z_{ini})^{-2}/4$, at $z_{ini} = 2000$, then Eq. (8) can be numerically solved. Substituting the results of Eq. (8) into Eq. (3), the key function $E(z)$ can be obtained. Notice that once n is given, $\Omega_{m0} = 1 - \Omega_{de}(0)$ can be naturally obtained by solving Eq. (8), so the ADE model is a single-parameter model.

B. Two-parameter models

(4) The XCDM model: DE has a constant EOS w , then

$$E(z) = \sqrt{\Omega_{m0}(1+z)^3 + (1 - \Omega_{m0})(1+z)^{3(1+w)}}. \quad (9)$$

(5) The Chaplygin gas (CG) model: The EOS of DE has the form [Kamenshchik et al. 2001]

$$p_{de} = -\frac{A}{\rho_{de}}, \quad (10)$$

where A is a positive constant, and p_{de} is the pressure of DE. From this assumption, one can get [Kamenshchik et al. 2001]

$$E(z) = \sqrt{\Omega_{m0}(1+z)^3 + (1-\Omega_{m0})\sqrt{A_c + (1-A_c)(1+z)^6}}, \quad (11)$$

here $A_c = A/\rho_{de}(0)$ is also a positive constant.

(6) The holographic dark energy (HDE) model: The DE density is characterized by the future event horizon L of the universe [Li 2004],

$$\rho_{de} = 3c^2 M_{Pl}^2 L^{-2}, \text{ and } L = a \int_t^\infty \frac{dt'}{a} = a \int_a^\infty \frac{da'}{H a'^2}, \quad (12)$$

where c is a positive constant. The equation of motion for Ω_{de} is given by [Li 2004]

$$\frac{d\Omega_{de}}{dz} = -(1+z)^{-1} \Omega_{de} (1 - \Omega_{de}) \left(1 + \frac{2}{c} \sqrt{\Omega_{de}} \right). \quad (13)$$

Solving Eq. (13) numerically and substituting the corresponding results into Eq. (3), $E(z)$ can be obtained.

(7) The holographic Ricci dark energy (RDE) model: The DE density is characterized by the Ricci scalar \mathcal{R} [Gao et al. 2009],

$$\rho_{de} = -\frac{\alpha}{16\pi G} \mathcal{R}, \text{ and } \mathcal{R} = -6 \left(\dot{H} + 2H^2 \right), \quad (14)$$

where α is a positive constant. The form of $E(z)$ in this case is [Gao et al. 2009]

$$E(z) = \sqrt{\frac{2\Omega_{m0}}{2-\alpha}(1+z)^3 + \left(1 - \frac{2\Omega_{m0}}{2-\alpha}\right)(1+z)^{(4-\frac{2}{\alpha})}}. \quad (15)$$

C. Three-parameter models

(8) The linear parameterization (LP) model: The EOS of DE is parameterized as

$$w = w_0 + w_1 z, \quad (16)$$

where w_0 and w_1 are constants. Then

$$E(z) = \sqrt{\Omega_{m0}(1+z)^3 + (1-\Omega_{m0})(1+z)^{3(1+w_0-w_1)} \exp(3w_1 z)}. \quad (17)$$

(9) The Chevallier-Polarski-Linder (CPL) model: The EOS of DE is parameterized as [Chevallier and Polarski 2001, Linder 2003]

$$w = w_0 + w_1 \frac{z}{1+z}, \quad (18)$$

then

$$E(z) = \sqrt{\Omega_{m0}(1+z)^3 + (1-\Omega_{m0})(1+z)^{3(1+w_0+w_1)} \exp\left(-\frac{3w_1 z}{1+z}\right)}. \quad (19)$$

(10) The generalized Chaplygin gas (GCG) model: The EOS of DE has the following form [Bento et al. 2002]

$$p_{de} = -\frac{A}{\rho_{de}^\alpha}, \quad (20)$$

where α is also a positive constant and $\alpha = 1$ corresponds to the CG model. One can get [Bento et al. 2002]

$$E(z) = \sqrt{\Omega_{m0}(1+z)^3 + (1-\Omega_{m0}) \left(A_s + (1-A_s)(1+z)^{3(1+\alpha)} \right)^{1/1+\alpha}}. \quad (21)$$

here $A_s = A/\rho_{de}^{1+\alpha}(0)$.

III. METHODOLOGY

A. Data analysis

In this work we adopt χ^2 statistics. For a physical quantity ξ with experimentally measured value ξ_{obs} , standard deviation σ_ξ , and theoretically predicted value ξ_{th} , the χ^2 value is given by

$$\chi_\xi^2 = \frac{(\xi_{th} - \xi_{obs})^2}{\sigma_\xi^2}. \quad (22)$$

The total χ^2 is the sum of all $\chi_{\xi^s}^2$, i.e.

$$\chi^2 = \sum_{\xi} \chi_\xi^2. \quad (23)$$

First, we consider the SNIa data that are given in terms of the distance modulus $\mu_{obs}(z_i)$. The theoretical distance modulus is defined as

$$\mu_{th}(z_i) \equiv 5 \log_{10} D_L(z_i) + \mu_0, \quad (24)$$

where $\mu_0 \equiv 42.38 - 5 \log_{10} h$ with h the Hubble constant H_0 in units of 100 km/s/Mpc, and in a flat universe the Hubble-free luminosity distance $D_L \equiv H_0 d_L$ (d_L denotes the physical luminosity distance) is

$$D_L(z) = (1+z) \int_0^z \frac{dz'}{E(z'; \theta)}, \quad (25)$$

where θ denotes the model parameters. The χ^2 for the SNIa data is

$$\chi_{SN}^2(\theta) = \sum_{i=1} \frac{[\mu_{obs}(z_i) - \mu_{th}(z_i; \theta)]^2}{\sigma_i^2}, \quad (26)$$

where $\mu_{obs}(z_i)$ and σ_i are the observed value and the corresponding 1σ error of distance modulus for each supernova, respectively. Parameter μ_0 is a nuisance parameter but it is independent of the data and the dataset. Following [Perivolaropoulos 2005], the minimization with respect to μ_0 can be made trivially by expanding the χ^2 of Eq. (26) with respect to μ_0 as

$$\chi_{SN}^2(\theta) = A(\theta) - 2\mu_0 B(\theta) + \mu_0^2 C, \quad (27)$$

where

$$A(\theta) = \sum_i \frac{[\mu_{obs}(z_i) - \mu_{th}(z_i; \mu_0 = 0, \theta)]^2}{\sigma_i^2}, \quad (28)$$

$$B(\theta) = \sum_i \frac{\mu_{obs}(z_i) - \mu_{th}(z_i; \mu_0 = 0, \theta)}{\sigma_i^2}, \quad (29)$$

$$C = \sum_i \frac{1}{\sigma_i^2}. \quad (30)$$

Evidently, Eq. (26) has a minimum for $\mu_0 = B/C$ at

$$\tilde{\chi}_{SN}^2(\theta) = A(\theta) - \frac{B(\theta)^2}{C}. \quad (31)$$

Since $\chi_{SN, min}^2 = \tilde{\chi}_{SN, min}^2$, instead of minimizing χ_{SN}^2 we will minimize $\tilde{\chi}_{SN}^2$ which is independent of the nuisance parameter μ_0 .

Next, we consider constraints from the CMB and the LSS observations. For the CMB data, we use the CMB shift parameter R , given by [Bond et al. 1997, Wang and Mukherjee 2006]

$$R \equiv \Omega_{m0}^{1/2} \int_0^{z_{rec}} \frac{dz'}{E(z')}, \quad (32)$$

where the redshift of recombination $z_{rec} = 1091.3$ [Komatsu et al. 2010]. The measured value of R has been updated to be $R_{obs} = 1.725 \pm 0.018$ from the WMAP7 observations [Komatsu et al. 2010]. For the LSS data, we use the BAO distance measurements obtained at $z = 0.2$ and $z = 0.35$ from the joint analysis of the 2dFGRS and SDSS data [Percival 2009]. The BAO distance ratio $D_V(z = 0.35)/D_V(z = 0.20) = 1.736 \pm 0.065$ was shown in [Percival 2009] to be a relatively model independent quantity. Here $D_V(z)$ is defined as

$$D_V(z_{BAO}) = \left[\frac{z_{BAO}}{H(z_{BAO})} \left(\int_0^{z_{BAO}} \frac{dz}{H(z)} \right)^2 \right]^{1/3}. \quad (33)$$

The total χ^2 is given by

$$\chi^2 = \tilde{\chi}_{SN}^2 + \chi_{CMB}^2 + \chi_{BAO}^2, \quad (34)$$

where $\tilde{\chi}_{SN}^2$ is given by Eq. (31), and the latter two terms are defined as

$$\chi_{CMB}^2 = \frac{(R - 1.725)^2}{0.018^2}, \quad (35)$$

and

$$\chi_{BAO}^2 = \frac{(D_V(0.35)/D_V(0.20) - 1.736)^2}{0.065^2}. \quad (36)$$

The model parameters yielding a minimal χ^2 is favored by the observations.

To compare different models, a statistical variable must be chosen. The χ_{min}^2 is the simplest one, but it has difficulty to compare different models with different number of parameters. In this work, we will use χ_{min}^2/dof as a model selection criterion, where dof is the degree of freedom defined as

$$dof \equiv N - k, \quad (37)$$

here N is the number of data, and k is the number of free parameters. This model selection criterion has been widely used in the literature.

B. SNIa Datasets

Although today there are many observational methods, SNIa is still one of the most powerful tools to probe the mysterious DE. In the past decade, many SNIa datasets have been released, while the number and quality of SNIa have continually increased. In 2008, the Union dataset [Kowalski et al. 2008] was released. It includes the large samples of SNIa from the HST, SNLS and ESSENCE, and contains 307 samples: 250 high redshift SNIa ($z > 0.2$) and 57 low redshift SNIa ($z \leq 0.2$). In 2009, the Constitution set [Hicken et al. 2009] was released. It adds 90 low redshift samples. These two SNIa datasets have been widely used in the literature.

In a recent work [Wei 2010], by comparing the maximum likelihood fits of the CPL parameters (w_0, w_1), Wei pointed out that both Union and Constitution datasets are in tension not only with the observations of CMB and BAO, but also with the other SNIa datasets. Moreover, he also investigated how to remove these tensions. The method of Wei is as follows. First, he fitted the Λ CDM model to all the data points in the specific SNIa dataset, and obtained the best-fit parameter value of Λ CDM model (for SNIa data only). Then, he calculated the relative deviation to the best-fit Λ CDM prediction, $|\mu_{obs} - \mu_{\Lambda CDM}|/\sigma_{obs}$, for all the SNIa data points. By searching the SNIa samples satisfying $|\mu_{obs} - \mu_{\Lambda CDM}|/\sigma_{obs} > 1.9$, Wei get the main sources that are responsible for the tensions. For the Union set, there are 21 SNIa differing from the best-fit Λ CDM prediction beyond 1.9σ , which is called ‘‘UnionOut’’ subset.

- **UnionOut subset (21 SNIa):**

1992bs, 1995ac, 1999bm, 1997o, 2001hu, 1998ba, 04Pat, 05Red, 2002hr, 03D4au, 04D3cp, 03D1fc, 03D4dy, 03D1co, b010, d033, g050, g055, k430, m138, m226

TABLE I: The “UnionOut” samples that satisfying $|\mu_{obs} - \mu_{model}|/\sigma_{obs} > 1.9$, for each model. Here “+” denotes adding a data point, while “-” denotes reducing a data point.

Model	Numbers of “UnionOut” samples for each model	Differences with the Λ CDM UnionOut subset						
Λ CDM	21	None						
DGP	21	None						
ADE	21	None						
XCDM	22	+1999gd	+f076	-05Red				
CG	22	+1999gd	+f076	-05Red				
HDE	22	+1999gd	+f076	-05Red				
RDE	22	+1999gd	+f076	-05Red				
LP	19	+1999gd	+f076	-1999bm	-05Red	-03D1co	-k430	
CPL	20	+1999gd	+f076	-1999bm	-05Red	-03D1co		
GCG	22	+1999gd	+f076	-05Red				

For the Constitution set, There are 34 SNIa differing from the best-fit Λ CDM prediction beyond 1.9σ , which is called “ConstitutionOut” subset.

- **ConstitutionOut subset (34 SNIa):**

1992bs, 1992bp, 1995ac, 1999bm, 1996t, 1997o, 1995aq, 2001hu, 1998ba, 04Pat, 05Red, 2002hr, 03D4au, 04D3gt, 04D3cp, 03D4at, 03D1fc, 04D3co, 03D4dy, 04D3oe, 04D1ak, 03D1co, b010, d033, f076, g050, k430, m138, m226, sn01cp, sn02hd, sn03ic, sn07ca, sn07R

It should be mentioned that 1.9σ is chosen based on two considerations: first, the tension between SNIa samples and other observations can be completely removed; second, the number of usable SNIa can be preserved as much as possible. After taking into account these two factors, Wei found that 1.9σ is most appropriate for the truncation procedure. By subtracting these two subsets from the Union dataset and the Constitution dataset, respectively, two new SNIa samples, “UnionT” and “ConstitutionT”, were obtained. It is clear that UnionT has 286 SNIa samples, and ConstitutionT has 363 SNIa samples. Analyzing these two truncated datasets with CPL model, Wei [Wei 2010] argued that they are fully consistent with the other cosmological observations.

But in [Wei 2010], only the Λ CDM model is used to select the outliers from the Union and the Constitution dataset. Since different DE models may select different outliers (i.e. different “UnionOut” and “ConstitutionOut” Samples), one may doubt whether the approach adopted in [Wei 2010] is valid. In principle, the truncation procedure should be performed for each different DE model. Only if the impact of different models is negligible, one can conclude that the conclusion of Wei is correct. So in this work, we perform the truncation procedure for 10 different DE models. As in [Wei 2010], we choose 1.9σ as the selection criterion. The results are shown in table I and table II. From these two tables, it is seen that the difference among the outlier samples given by various models are very small, and the impact of different models is negligible. Therefore, the approach adopted in [Wei 2010] is valid. Since the difference among the outlier samples given by various models are very small, for simplicity, in this work we just adopt the UnionT and the ConstitutionT SNIa samples given by [Wei 2010]. To explore the corresponding cosmological consequences, in the following we shall study 10 models by using 4 SNIa datasets: Union, UnionT, Constitution and ConstitutionT.

IV. RESULTS AND CONCLUSIONS

We will present the results of data fitting in this section. Using the Union, the UnionT, the Constitution and the ConstitutionT dataset, respectively, we list the χ^2_{min} and the χ^2_{min}/dof for those 10 models, in table III, table IV, table V, and table VI. Here “SNIa” means only SNIa data is used in the analysis, “SNIa+BAO” means both SNIa data and BAO data are used, “SNIa+CMB” means both SNIa data and CMN data are used, and “SNIa+BAO+CMB” means all these three types of observational data are taken into account. The main conclusions are summarized as follows.

(1) For each DE model, the truncated SNIa datasets not only greatly reduce χ^2_{min} and χ^2_{min}/dof , but also remove the tension between SNIa data and other cosmological observations.

TABLE II: The ‘‘ConstitutionOut’’ samples that satisfying $|\mu_{obs} - \mu_{model}|/\sigma_{obs} > 1.9$, for each model. Here ‘‘+’’ denotes adding a data point, while ‘‘-’’ denotes reducing a data point.

Model	Numbers of ‘‘ConstitutionOut’’ samples for each model	Difference with the Λ CDM ConstitutionOut subset			
Λ CDM	34	None			
DGP	34	None			
ADE	33	-sn07R			
XCDM	34	None			
CG	34	+1997aj -1992bp			
HDE	34	None			
RDE	34	None			
LP	32	+1997aj	-1992bp	-1999bm	-03D4at
CPL	33	+1997aj	+sn02bf	-1992bp	-1999bm -sn07R
GCG	34	+1997aj -1992bp			

TABLE III: The χ^2_{min} and the χ^2_{min}/dof (in the Parentheses) for the 10 models, where the Union dataset is used.

Model	SNIa	SNIa+BAO	SNIa+CMB	SNIa+BAO+CMB
Λ CDM	311.936 (1.019)	313.205 (1.020)	312.424 (1.018)	313.594 (1.018)
DGP	313.026 (1.023)	314.319 (1.024)	339.280 (1.105)	341.584 (1.109)
ADE	313.536 (1.025)	314.838 (1.026)	327.216 (1.066)	329.252 (1.069)
XCDM	310.682 (1.019)	311.966 (1.020)	312.224 (1.020)	313.456 (1.021)
CG	310.434 (1.018)	311.628 (1.018)	311.921 (1.019)	313.193 (1.020)
HDE	310.827 (1.019)	312.149 (1.020)	311.218 (1.017)	312.481 (1.018)
RDE	310.682 (1.019)	311.966 (1.020)	312.323 (1.021)	313.801 (1.022)
LP	309.984 (1.020)	310.744 (1.019)	310.691 (1.019)	311.978 (1.020)
CPL	310.091 (1.020)	310.896 (1.019)	310.906 (1.019)	312.258 (1.020)
GCG	310.405 (1.021)	311.401 (1.021)	311.925 (1.023)	313.325 (1.024)

TABLE IV: The χ^2_{min} and the χ^2_{min}/dof (in the Parentheses) for the 10 models, where the UnionT dataset is used.

Model	SNIa	SNIa+BAO	SNIa+CMB	SNIa+BAO+CMB
Λ CDM	204.568 (0.718)	205.945 (0.720)	205.575 (0.719)	206.794 (0.721)
DGP	205.234 (0.720)	206.634 (0.722)	226.987 (0.794)	229.388 (0.799)
ADE	205.560 (0.721)	206.963 (0.724)	216.201 (0.756)	218.305 (0.761)
XCDM	204.058 (0.719)	205.449 (0.721)	204.855 (0.719)	206.207 (0.721)
CG	204.050 (0.718)	205.365 (0.721)	204.552 (0.718)	205.930 (0.720)
HDE	204.070 (0.719)	205.496 (0.721)	204.228 (0.717)	205.614 (0.719)
RDE	204.058 (0.719)	205.449 (0.721)	205.875 (0.722)	207.498 (0.726)
LP	204.055 (0.721)	205.347 (0.723)	204.429 (0.720)	205.739 (0.722)
CPL	204.057 (0.721)	205.391 (0.723)	204.063 (0.719)	205.517 (0.721)
GCG	204.053 (0.721)	205.366 (0.723)	204.545 (0.720)	206.090 (0.723)

TABLE V: The χ_{min}^2 and the χ_{min}^2/dof (in the Parentheses) for the 10 models, where the Constitution dataset is used.

Model	SNIa	SNIa+BAO	SNIa+CMB	SNIa+BAO+CMB
Λ CDM	465.604 (1.176)	466.902 (1.176)	466.316 (1.175)	467.525 (1.175)
DGP	466.122 (1.177)	467.433 (1.177)	498.264 (1.255)	500.368 (1.257)
ADE	466.275 (1.177)	467.580 (1.178)	483.675 (1.218)	485.585 (1.220)
XCDM	465.602 (1.179)	466.901 (1.179)	465.657 (1.176)	466.947 (1.176)
CG	465.293 (1.178)	466.564 (1.178)	465.591 (1.176)	466.891 (1.176)
HDE	465.769 (1.179)	467.080 (1.179)	466.030 (1.177)	467.384 (1.177)
RDE	465.602 (1.179)	466.901 (1.179)	472.841 (1.194)	474.466 (1.195)
LP	461.071 (1.170)	461.570 (1.169)	465.610 (1.179)	466.910 (1.179)
CPL	461.526 (1.171)	462.112 (1.170)	465.636 (1.179)	466.902 (1.179)
GCG	465.080 (1.180)	466.360 (1.181)	465.920 (1.180)	466.895 (1.179)

TABLE VI: The χ_{min}^2 and the χ_{min}^2/dof (in the Parentheses) for the 10 models, where the ConstitutionT dataset is used.

Model	SNIa	SNIa+BAO	SNIa+CMB	SNIa+BAO+CMB
Λ CDM	269.081 (0.743)	270.610 (0.745)	271.423 (0.748)	272.764 (0.749)
DGP	269.443 (0.744)	270.979 (0.747)	292.067 (0.805)	294.360 (0.809)
ADE	269.613 (0.745)	271.139 (0.747)	280.090 (0.772)	282.147 (0.775)
XCDM	269.066 (0.745)	270.599 (0.748)	269.245 (0.744)	270.754 (0.746)
CG	268.992 (0.745)	270.502 (0.747)	269.066 (0.743)	270.594 (0.745)
HDE	269.113 (0.745)	270.664 (0.748)	269.130 (0.743)	270.698 (0.746)
RDE	269.066 (0.745)	270.599 (0.748)	273.305 (0.755)	275.180 (0.758)
LP	268.812 (0.747)	270.021 (0.748)	269.068 (0.745)	270.603 (0.748)
CPL	268.900 (0.747)	270.147 (0.748)	269.122 (0.745)	270.676 (0.748)
GCG	268.980 (0.747)	270.473 (0.749)	269.069 (0.745)	270.599 (0.748)

Since it is too prolix to describe the results of all 10 models, in the following we will just discuss the HDE model as an example. From table III and table IV, we can see that the combined Union+BAO+CMB data gives a $\chi_{min}^2 = 312.481$ and a $\chi_{min}^2/dof = 1.018$, while the combined UnionT+BAO+CMB data gives a $\chi_{min}^2 = 205.614$ and a $\chi_{min}^2/dof = 0.719$. This means that by dropping the 21 outliers, The χ_{min}^2 and the χ_{min}^2/dof of the HDE model can reduce 106.867 and 0.299, respectively. From table V and table VI, similar results are obtained. The combined Constitution+BAO+CMB data gives a $\chi_{min}^2 = 467.384$ and a $\chi_{min}^2/dof = 1.177$, while the combined ConstitutionT+BAO+CMB data gives a $\chi_{min}^2 = 270.698$ and a $\chi_{min}^2/dof = 0.746$. This means that by dropping the 34 outliers, The χ_{min}^2 and the χ_{min}^2/dof of the HDE model can reduce 196.686 and 0.431, respectively. It should be pointed out that for all these 10 models, the UnionT and the ConstitutionT dataset can greatly reduce the corresponding χ_{min}^2 and χ_{min}^2/dof . Moreover, the decreasing margin of χ_{min}^2 and χ_{min}^2/dof for these 10 DE models are almost same.

To further verify this conclusion, we also adopt the method of random truncation used in [Nesseris and Perivolaropoulos 2007, Wei 2010]. The method is very simple. First, we random select the outliers from the full Union dataset and the full Constitution dataset, respectively. Notice that the numbers of data points in these random ‘‘UnionOut’’ subsets are same as that in the original UnionOut samples, while the numbers of data points in these random ‘‘ConstitutionOut’’ subsets are same as that in the original ConstitutionOut samples. As in [Nesseris and Perivolaropoulos 2007, Wei 2010], 500 random UnionOut subsets and 500 random ConstitutionOut subsets are selected. By subtracting these outliers from the Union dataset and the Constitution dataset, respectively, 500 random UnionT subsets and 500 random ConstitutionT subsets are obtained. Then, we perform best-fit analysis on the HDE model by using these random truncated SNIa subsets. Using the SNIa data only, we get the Mean of χ_{min}^2 for 500 random UnionOut subsets and 500 random ConstitutionOut subsets, respectively. Notice that the full Union set gives a $\chi_{min}^2 = 310.827$ and the full Constitution set gives a $\chi_{min}^2 = 465.769$, the differences between

TABLE VII: A comparison for the original truncated SNIa subset and the random truncated SNIa subsets. Notice that the full Union set gives a $\chi_{min}^2 = 310.827$ and the full Constitution set gives a $\chi_{min}^2 = 465.769$. Here ΔN is the number of data points in outliers, $\overline{\chi^2}$ is the Mean of χ_{min}^2 for those random truncated SNIa subsets, and $\Delta\chi^2$ is the differences between the χ_{min}^2 of the full SNIa dataset and the χ_{min}^2 (or the Mean) of the random truncated SNIa subsets.

The subset of outliers	ΔN	χ_{min}^2 or $\overline{\chi^2}$	$\Delta\chi^2$	$\Delta\chi^2/\Delta N$
The original UnionOut subset	21	204.070	106.757	5.084
500 random UnionOut subsets	21 (Mean)	289.617 (Mean)	21.210 (Mean)	1.010 (Mean)
The original ConstitutionOut subset	34	269.113	199.656	5.784
500 random ConstitutionOut subsets	34 (Mean)	425.763 (Mean)	40.006 (Mean)	1.177 (Mean)

the χ_{min}^2 of the full SNIa dataset and the Mean of χ_{min}^2 of these random truncated SNIa subsets are also obtained. Next, we make a comparison for the original truncated SNIa subset and the random truncated SNIa subsets. The results are shown in table VII. It is found that the χ_{min}^2 of the HDE model can reduce 5 by dropping 1 data point in the original truncated SNIa subset, but can only reduce 1 by dropping 1 data point in the random truncated SNIa subset. Therefore, the original UnionOut and ConstitutionOut subsets are systematically different from the full Union and Constitution datasets, and the original truncated supernova datasets provide a significantly better model fitting than the full SNIa datasets.

In [Wei 2010], by performing the best-fit analysis on the CPL model, Wei argued that the UnionT and the ConstitutionT datasets are fully consistent with the other cosmological observations. To verify this conclusion, more theoretical models should be taken into account. Here we study the HDE model as an example. In Fig.1, we plot the 1σ and the 2σ confidence level (CL) contours for the HDE model, where the Union and the UnionT datasets are used, respectively. From this figure, we find that the best-fit point for the Union data is outside the 2σ confidence region given by the combined Union+BAO+CMB data, while the best-fit point for the UnionT data is inside the 1σ confidence region given by the combined UnionT+BAO+CMB data. This means that the UnionT dataset is very useful to remove the tension between SNIa data and other cosmological observations. In addition, we also use the Constitution and the ConstitutionT datasets to plot the CL contours for the HDE model in Fig.2. It is found that the best-fit point for the Constitution data is outside the 2σ confidence region given by the combined Constitution+BAO+CMB data, while the best-fit point for the ConstitutionT data is very close to the best-fit point for the combined ConstitutionT+BAO+CMB data. This means that the ConstitutionT dataset is also very helpful to remove the tension. Therefore, we conclude that the truncated SNIa datasets can remove the tension between SNIa data and other cosmological observations.

(2) The CMB data is very helpful to break the degeneracy among different parameters, and plays a very important role in distinguishing different DE models.

As an example, we will compare the HDE model with the RDE model. By using the Constitution SNIa data alone, the CMB data alone, and the combined Constitution+CMB+BAO data, respectively, we plot the 1σ and the 2σ CL contours for the HDE and the RDE model in Fig.3. From this figure, we find that the shapes of CL contours given by the CMB data alone are quite different from that given by the SNIa data alone, and the CMB data is very helpful to break the degeneracy among different parameters. As shown in the left panel, the 1σ CL contour of the HDE model given by the CMB data intersects to the 1σ CL contour of the HDE model given by the SNIa data; while in the right panel, the 1σ CL contour of the RDE model given by the CMB data does not intersect to the 1σ CL contour of the RDE model given by the SNIa data. This fact explains why the HDE model performs much better in fitting the combined Constitution+BAO+CMB data than the RDE model. Besides, we also check the effect of the BAO data, and find that the 1σ confidence region of the HDE model given by the BAO data alone can completely cover that given by the SNIa data. So the constraint given by the BAO data is quite weaker than that given by the SNIa and the BAO data. This conclusion can be further verified by using table V. As seen in table V, without adopting the CMB data, it is very difficult to distinguish the HDE Model from the RDE model. After adding the CMB data, it is seen that the χ_{min}^2 of the HDE Model given by the SNIa+CMB data is 6.811 smaller than the χ_{min}^2 of the RDE Model given by the SNIa+CMB data, while the χ_{min}^2 of the HDE Model given by the combined SNIa+CMB+BAO data is 7.082 smaller than the χ_{min}^2 of the RDE Model given by the combined SNIa+CMB+BAO data.

In addition, by using the ConstitutionT SNIa data alone, the CMB data alone, and the combined ConstitutionT+CMB+BAO data, respectively, we also plot the 1σ and the 2σ CL contours for the HDE and the RDE model in Fig.4. Again, we see that the 1σ CL contour of the HDE model given by the CMB data intersects to the 1σ CL contour of the HDE model given by the SNIa data, while the 1σ CL contour of the RDE model given by the CMB data does not intersect to the 1σ CL contour of the RDE model given by the SNIa data. This fact explains

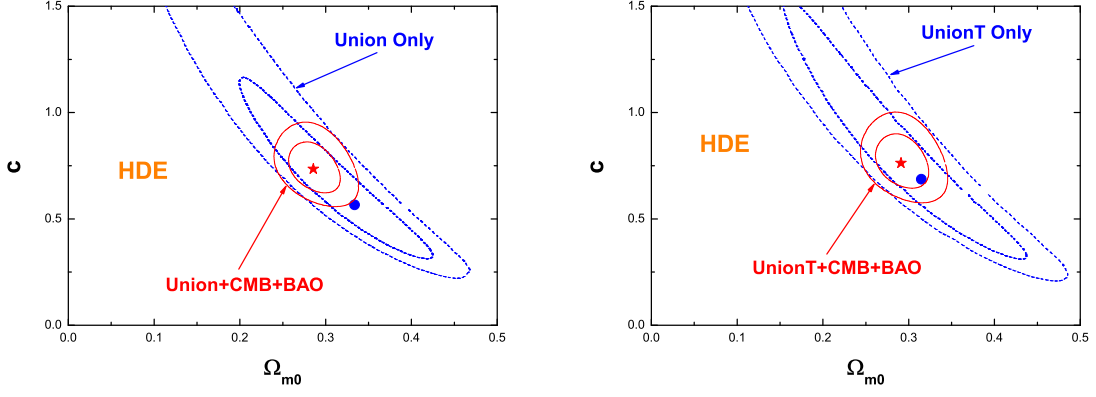


FIG. 1: The 1σ and the 2σ CL contours for the HDE model. The left panel is plotted by using the Union dataset, while the right panel is plotted by using the UnionT dataset. For both these two panels, the blue dashed lines correspond to the constraints given by the SNIa data only, and the red solid lines correspond to the constraints given by the combined SNIa+BAO+CMB data. Moreover, we also plot the best-fit point for the SNIa data (blue point) and the best-fit point for the combined SNIa+BAO+CMB data (red star). It should be pointed out that, in the left panel, the best-fit point for the SNIa data is outside the 2σ confidence region given by the combined SNIa+BAO+CMB data, while in the right panel, the best-fit point for the SNIa data is inside the 1σ confidence region given by the combined SNIa+BAO+CMB data. This means that the UnionT dataset is very useful to remove the tension between SNIa data and other cosmological observations.

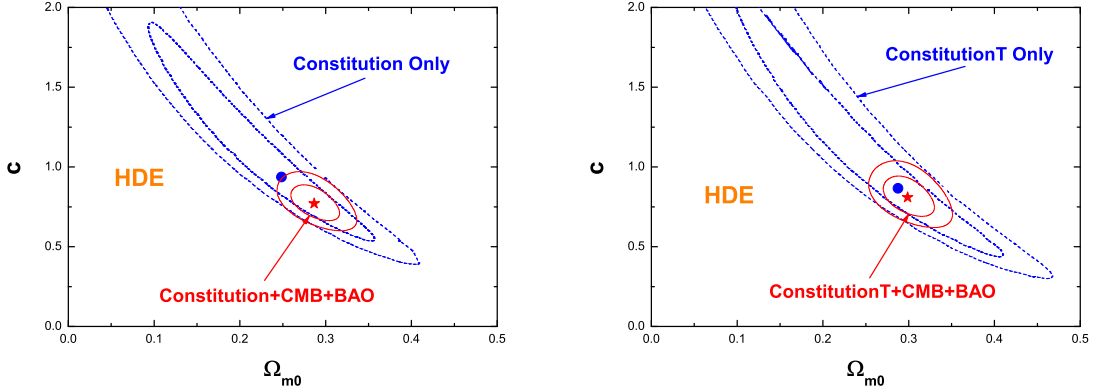


FIG. 2: The same as in Fig.1, except for the cases of the Constitution and the ConstitutionT datasets. It should be mentioned that, in the left panel, the best-fit point for the SNIa only is outside the 2σ confidence region given by the combined SNIa+BAO+CMB data, while in the right panel, the best-fit point for the SNIa only is very close to the best-fit point for the combined SNIa+BAO+CMB data. This means that the ConstitutionT dataset is very helpful to remove the tension between SNIa data and other cosmological observations.

why the HDE model performs much better in fitting the combined ConstitutionT+BAO+CMB data than the RDE model. Therefore, the CMB data is very helpful to break the degeneracy among different parameters, and plays a very important role in distinguishing different DE models.

(3) The current observational data are still too limited to distinguish all DE models.

First, we discuss three kinds of two-parameter models: the Λ CDM model, the CG model, and the HDE model. As seen in table V, the χ^2_{min} of these 3 models given by the combined Constitution+BAO+CMB data are 466.947, 466.891, and 467.384, respectively. That is to say, after taking into account the CMB data, the differences of the χ^2_{min} of these 3 models are still smaller than 1. Notice that this result also holds true in table III, table IV, and table VI. Therefore, one cannot judge which DE model is better.

Then, we discuss three kinds of three-parameter models: the LP model, the CPL model, and the GCG model. As seen in table V, the χ^2_{min} of these 3 models given by the combined Constitution+BAO+CMB data are 466.910,

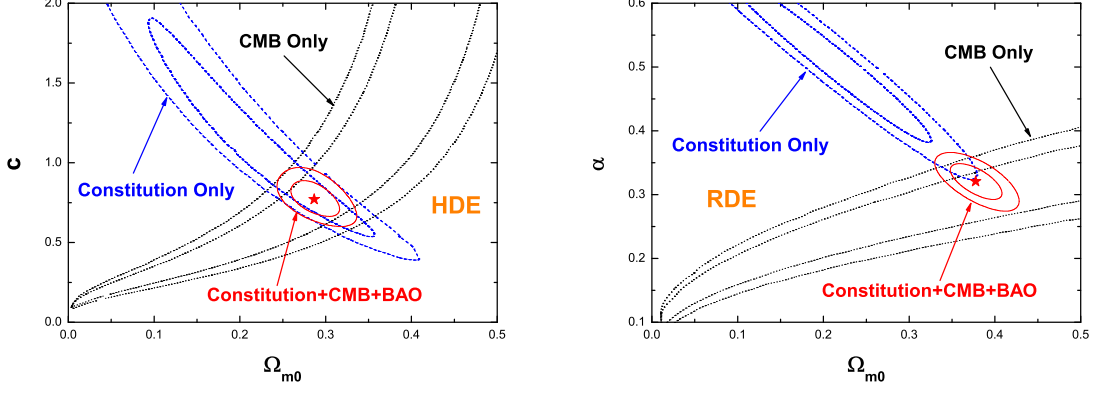


FIG. 3: The 1σ and the 2σ CL contours for the HDE and the RDE model. The Constitution dataset is used to plot this figure. The left panel is plotted by using the HDE model, while the right panel is plotted by using the RDE model. For both these two panels, The blue dashed lines correspond to the constraints given by the SNIa data only, the black dotted lines correspond to the constraints given by the CMB data only, the red solid lines correspond to the constraints given by the combined SNIa+BAO+CMB data, and the red stars denote the best-fit point for the combined SNIa+BAO+CMB data. Since the shapes of CL contours given by the CMB data alone are quite different from that given by the SNIa data alone, the CMB data is very helpful to break the degeneracy among different parameters. As shown in the left panel, the 1σ CL contour of the HDE model given by the CMB data intersects to the 1σ CL contour of the HDE model given by the SNIa data; while in the right panel, the 1σ CL contour of the RDE model given by the CMB data does not intersect to the 1σ CL contour of the RDE model given by the SNIa data. This fact explains why the HDE model performs much better in fitting the combined Constitution+BAO+CMB data than the RDE model. Besides, we also check the effect of the BAO data, and find that the 1σ confidence region of the HDE model given by the BAO data alone can completely cover that given by the SNIa data. For simplicity, the CL contours given by the BAO data are not plotted in this figure.

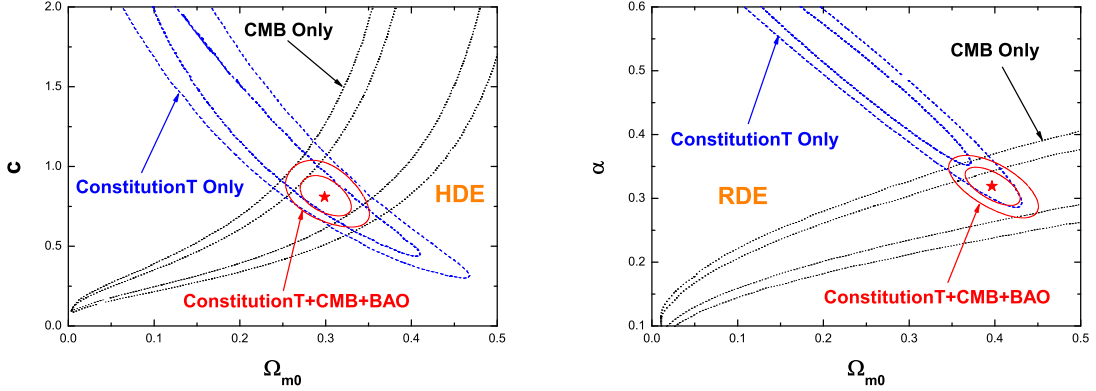


FIG. 4: The same as in Fig.3, except for the case of the ConstitutionT dataset. Notice that the shapes of CL contours given by the CMB data alone are quite different from that given by the SNIa data alone. As shown in the left panel, the 1σ CL contour of the HDE model given by the CMB data intersects to the 1σ CL contour of the HDE model given by the SNIa data; while in the right panel, the 1σ CL contour of the RDE model given by the CMB data does not intersect to the 1σ CL contour of the RDE model given by the SNIa data. This fact explains why the HDE model performs much better in fitting the combined ConstitutionT+BAO+CMB data than the RDE model.

466.902, 466.895, respectively, and the differences of the χ^2_{min} of these 3 models are even smaller than 0.1. Since this result also holds true in table III, table IV, and table VI, it is also very difficult to distinguish these 3 models. Therefore, to distinguish DE models better, more high-quality observational data are needed.

V. SUMMARY

In this work, by performing the truncation procedure of [Wei 2010] for 10 different models, we demonstrate that the approach adopted in [Wei 2010] is valid. Moreover, by using the 4 SNIa datasets mentioned above, as well as the observations of CMB and BAO, we perform best-fit analysis on the 10 DE models. It is found that: (1) For each DE model, the truncated SNIa datasets not only greatly reduce χ_{min}^2 and χ_{min}^2/dof , but also remove the tension between SNIa data and other cosmological observations. (2) The CMB data is very helpful to break the degeneracy among different parameters, and plays a very important role in distinguishing different DE models. (3) The current observational data are still too limited to distinguish all DE models. These results provide a further support for Wei's work, and indicate that the existence of biasing systematic errors in SNIa data should be taken into account seriously.

Acknowledgements

We are grateful to the reviewer for very useful and helpful suggestions. We also thank Qing-Guo Huang, Hao Wei and Xin Zhang, for helpful discussions. This work was supported by the NSFC grant No.10535060/A050207, a NSFC group grant No.10821504 and Ministry of Science and Technology 973 program under grant No.2007CB815401. Shuang Wang was also supported by a graduate fund of USTC.

-
- [Albrecht et al. 2006] Albrecht, A. et al., 2006, arXiv:astro-ph/0609591
 [Armendariz-Picon et al. 1999] Armendariz-Picon, C. et al., 1999, Phys. Lett. B 458, 209
 [Armendariz-Picon et al. 2001] Armendariz-Picon, C. et al., 2001, Phys. Rev. D 63, 103510
 [Astier et al. 2007] Astier, P. et al., 2007, Astron. Astrophys. 447, 31
 [Bagla et al. 2003] Bagla, J.S. et al., 2003, Phys. Rev. D 67, 063504
 [Bennet et al. 2003] Bennet, C.L. et al., 2003, ApJS. 148, 1
 [Bento et al. 2002] Bento, M.C. et al., 2002, Phys. Rev. D 66, 043507
 [Bond et al. 1997] Bond, J.R. et al., 1997, MNRAS. 291, L33
 [Caldwell 2002] Caldwell, R.R., 2002, Phys. Lett. B 545, 23
 [Carroll 2001] Carroll, S.M., 2001, Living Rev. Rel. 4, 1
 [Carroll et al. 2003] Carroll, S.M. et al., 2003, Phys. Rev. D 68, 023509
 [Chang et al. 2006] Chang, Z. et al., 2006, Phys. Lett. B 633, 14
 [Chen et al. 2009] Chen, C.W. et al., 2009, Phys. Lett. B 682 267
 [Chevallier and Polarski 2001] Chevallier, M. and Polarski, D., 2001, Int. J. Mod. Phys. D 10, 213
 [Chiba et al. 2000] Chiba, T. et al., 2000, Phys. Rev. D 62, 023511
 [Copeland et al. 2006] Copeland, E.J. et al., 2006, Int. J. Mod. Phys. D 15, 1753
 [Davis et al. 2007] Davis, T. et al., 2007, ApJ. 666, 716
 [Dvali et al. 2000] Dvali, G.R. et al., 2000, Phys. Lett. B 485, 208
 [Eisenstein et al. 2005] Eisenstein, D.J. et al., 2005 ApJ. 633, 560
 [Gao et al. 2009] Gao, C. et al., 2009, Phys. Rev. D 79, 043511
 [Gong and Li 2010a] Gong, Y.G. and Li, T.J., 2010, Phys. Lett. B 683 241
 [Gong et al. 2010b] Gong, Y.G. et al., 2010, JCAP 01 019
 [Hicken et al. 2009] Hicken, M. et al., 2009, ApJ 700, 1097
 [Hinshaw et al. 2007] Hinshaw, G. et al., 2007, ApJS 170, 263
 [Huang and Gong 2004] Huang, Q.G. and Gong, Y.G., 2004 JCAP 0408, 006
 [Huang and Li 2005a] Huang, Q.G. and Li, M., 2005, JCAP 0408, 013
 [Huang and Li 2005b] Huang, Q.G. and Li, M., 2005, JCAP 0503, 001
 [Huang et al. 2009] Huang, Q.G. et al., 2009, Phys. Rev. D 80 083515
 [Huterer and Starkman 2003] Huterer, D. and Starkman, G., 2003 Phys. Rev. Lett. 90, 031301
 [Huterer and Cooray 2005] Huterer, D. and Cooray, A., 2005, Phys. Rev. D 71, 023506
 [Jassal et al. 2005] Jassal, H. et al., 2005, Phys. Rev. D 72,103503
 [Jassal et al. 2006] Jassal, H. et al., 2006, arXiv:astro-ph/0601389, accepted for publication in MNRAS
 [Kamenshchik et al. 2001] Kamenshchik, A.Y. et al., 2001, Phys. Lett. B 511 265
 [Knop et al. 2003] Knop, R.A. et al., 2003, ApJ 598, 102
 [Komatsu et al. 2009] Komatsu, E. et al., 2009, ApJS. 180, 3301
 [Komatsu et al. 2010] Komatsu, E. et al., arXiv:1001.4538.
 [Kowalski et al. 2008] Kowalski, M. et al., 2008 ApJ. 686, 749
 [Li 2004] Li, M., 2004, Phys. Lett. B 603 1
 [Li et al. 2008] Li, M. et al., 2008, JCAP 0805, 023

- [Li et al. 2009a] Li, M. et al., 2009, *Commun. Theor. Phys.* 51, 181
- [Li et al. 2009b] Li, M. et al., 2009, *JCAP* 0906, 036
- [Linder 2003] Linder, E.V., 2003, *Phys. Rev. Lett.* 90, 091301
- [Ma et al. 2009a] Ma, Y.Z. et al., 2009, *Eur. Phys. J. C* 60, 303
- [Ma et al. 2009b] Ma, Y.Z. et al., 2009, arXiv:0901.1215
- [Mortonson et al. 2009] Mortonson, M.J. et al., 2009, *Phys. Rev. D* 80, 067301
- [Nesseris and Perivolaropoulos 2005] Nesseris, S. and Perivolaropoulos, L., 2005, *Phys. Rev. D* 72, 123519
- [Nesseris and Perivolaropoulos 2007] Nesseris, S. and Perivolaropoulos, L., 2007, *JCAP* 0702, 025
- [Padmanabhan 2002] Padmanabhan, T., 2002, *Phys. Rev. D* 66, 021301
- [Padmanabhan 2003] Padmanabhan, T., 2003, *Phys. Rept.* 380, 235
- [Page et al. 2007] Page, L. et al., 2007, *ApJS* 170, 335
- [Peebles and Ratra 1988] Peebles, P.J.E. and Ratra, B., 1988, *ApJL* 325, 17
- [Peebles and Ratra 2003] Peebles, P.J.E. and Ratra, B., 2003, *Rev. Mod. Phys.* 75, 559
- [Percival 2009] Percival, W.J. et al., 2009, arXiv:0907.1660, accepted for publication in *MNRAS*
- [Perivolaropoulos 2005] Perivolaropoulos, L., 2005 *Phys. Rev. D* 71, 063503
- [Perlmutter et al. 1999] Perlmutter, S. et al., 1999 *ApJ* 517, 565
- [Qi et al. 2009] Qi, S. et al., 2009, *MNRAS* 398 L78
- [Ratra and Peebles 1988] Ratra, B. and Peebles, P.J.E., 1988, *Phys. Rev. D* 37, 3406
- [Riess et al. 1998] Riess, A.G. et al., 1998 *AJ*. 116, 1009
- [Riess et al. 2004a] Riess, A.G. et al., 2004, *ApJ* 607, 665.
- [Riess et al. 2004b] Riess, A.G. et al., 2004, *ApJ*. 607, 665
- [Riess et al. 2007] Riess, A.G. et al., 2007, *ApJ*. 659, 98
- [Sahni and Starobinsky 2000] Sahni, V. and Starobinsky, A.A., 2000, *Int. J. Mod. Phys. D* 9, 373
- [Sanchez et al. 2009] Sanchez, J.C.B. et al., 2009, arXiv:0908.2636.
- [Shafieloo et al. 2009] Shafieloo, A. et al., 2009, *Phys. Rev. D (Rapid Communication)* 80, 101301
- [Spergel et al. 2003] Spergel, D.N. et al., 2003, *ApJS*, 148, 175
- [Spergel et al. 2007] Spergel, D.N. et al., 2007, *ApJS* 170, 377
- [Tegmark et al. 2004a] Tegmark, M. et al., 2004, *Phys. Rev. D* 69, 103501
- [Tegmark et al. 2004b] Tegmark, M. et al., 2004, *ApJ* 606, 702
- [Tegmark et al. 2006] Tegmark, M. et al., 2006, *Phys. Rev. D* 74, 123507
- [Tonry et al. 2003] Tonry, J. L. et al., 2003, *ApJ* 594, 1
- [Wang et al. 2005] Wang, B. et al., 2005, *Phys. Lett. B* 611, 21
- [Wang et al. 2006] Wang, B. et al., 2006, *Phys. Lett. B* 637, 357
- [Wang et al. 2008] Wang, S. et al., 2008, *JCAP* 10 037
- [Wang and Zhang 2008] Wang, S. and Zhang, Y., 2008, *Phys. Lett. B* 669 201
- [Wang et al. 2010] Wang, S. et al., 2010, arXiv:1005.4345
- [Wang 2000] Wang, Y., 2000 *ApJ*, 536, 531
- [Wang and Mukherjee 2004] Wang, Y. and Mukherjee, P., 2004, *ApJ*, 606, 654
- [Wang and Mukherjee 2006] Wang, Y. and Mukherjee, P., 2004, *ApJ*. 650, 1
- [Wang and Mukherjee 2007] Wang, Y. and Mukherjee, P., 2007, *Phys. Rev. D* 76, 103533
- [Wei et al. 2005] Wei, H. et al., 2005, *Class. Quant. Grav.* 22, 3189
- [Wei and Cai 2005] Wei, H. and Cai, R.G., 2005, *Phys. Rev. D* 72, 123507
- [Wei and Cai 2007] Wei, H. and Cai, R.G., 2007, *Phys. Lett. B* 655, 1
- [Wei and Cai 2008a] Wei, H. and Cai, R.G., 2008, *Phys. Lett. B* 660, 113
- [Wei and Cai 2008b] Wei, H. and Cai, R.G., 2008, *Phys. Lett. B* 663, 1
- [Wei and Cai 2008c] Wei, H. and Cai, R.G., 2008, *Phys. Lett. B* 663, 1
- [Wei and Cai 2009] Wei, H. and Cai, R.G., 2009, *Eur. Phys. J. C* 59, 99
- [Wei 2010] Wei, H., 2010, *Phys. Lett. B* 687, 286
- [Weinberg 1989] Weinberg, S., 1989, *Rev. Mod. Phys.* 61, 1
- [Weinberg 2000] Weinberg, S., 2000, arXiv:astro-ph/0005265
- [Wetterich 1988] Wetterich, C., 1988, *Nucl. Phys. B* 302, 668
- [Wood-Vasey et al. 2007] Wood-Vasey, W. et al., 2007, *ApJ*. 666, 694
- [Xia and Zhang 2007] Xia, T.Y. and Zhang, Y., 2007, *Phys. Lett. B* 656, 19
- [Zhang and Wu 2009] Zhang, Q.J. and Wu, Y.L., 2009, arXiv:0905.1234.
- [Zhang and Wu 2004] Zhang, X. and Wu, F.Q., 2005, *Phys. Rev. D* 72, 043524
- [Zhang 2005] Zhang, X., 2005, *Int. J. Mod. Phys. D* 14, 1597
- [Zhang 2007] Zhang, X., 2007, *Phys. Lett. B* 648, 1
- [Zhang and Wu 2007] Zhang, X. and Wu, F.Q., 2007, *Phys. Rev. D* 76, 023502
- [Zhang 2009] Zhang, X., 2009, *Phys. Rev. D* 79, 103509
- [Zhang 2010] Zhang, X., 2010, *Phys. Lett. B* 683, 81
- [Zhang et al. 2007] Zhang, Y. et al., 2007, *Class. Quant. Grav.* 24, 3309
- [Zlatev et al. 1999] Zlatev, I. et al., 1999, *Phys. Rev. Lett.* 82, 896